Noise-Robust Processing of Phase Dislocations using Combined Unwrapping and Sparse Inpainting with Dictionary Learning

Jesus Pineda*, Jhacson Meza*, Erik M. Barrios†, Lenny A. Romero‡, Andres G. Marrugo*
*Facultad de Ingenieria, Universidad Tecnologica de Bolivar, Cartagena, Colombia.
†Esc. Ciencias Basicas, Tecnologia e Ingenieria, Universidad Nacional Abierta y a Distancia, Corozal, Colombia.
‡Facultad de Ciencias Basicas, Universidad Tecnologica de Bolivar, Cartagena, Colombia.
jesuspinedacastro@outlook.com

***Abstract*—The problem of phase unwrapping from a noisy and also incomplete wrapped phase map arises in many optics and image processing applications. In this work, we propose a noise-robust approach for processing regional phase dislocations. Our approach combines phase unwrapping and sparse-based inpainting with dictionary learning to recover the continuous phase map. The method is validated both using numerically simulated data with strong additive white Gaussian noise and phase dislocations; and experimental data from fringe projection profilometry. Comparisons with other phase inpainting method referred to as PULSI+INTERP, show the suitability of the proposed method for phase restoration even in extremely noisy phases. The error given by the proposed method on the highest level of noise (RMSE=0.0269 Rad) remains the smallest compared to the error given by PULSI+INTERP for noise-free data (RMSE=0.0332 Rad).**

***Index Terms*—Phase Unwrapping, Image Restoration, 3-D Reconstruction, Dictionary Learning, Sparse representation**

I. Introduction

Phase unwrapping is a necessary process in many applications such as synthetic radar aperture, fringe projection profilometry, interferometry, magnetic resonance imaging, among others. The unwrapping process consists of retrieving the true continuous phase from its wrapped version, typically in the interval $(-\pi, \pi]$ as recovered using a phase recovery method [1]. Successful phase recovery occurs when the recovered wrapped phase is such that the maximum phase change between sample points is $< \pi$ [2]. When this condition is not met phase residues appear, which are associated with local inconsistencies of the phase map [3], [4]. These inconsistencies often arise in regions where the fringe pattern breaks due to structural discontinuities in the recovered wrapped phase leading to phase dislocations. In practice, we have to deal not only with phase dislocations but also with noise. These circumstances make phase unwrapping a difficult task and decreases the accuracy of the measurement.

Conventional phase unwrapping algorithms such as quality guided approaches [5], Flynn's minimum discontinuity [6], and minimum L^p-norm algorithms [7], have proven to be effective when dealing with noisy phase data, but not further with local dislocations [8], [9]. Recently, many algorithms have been proposed for effectively processing phase dislocations based on inpainting approaches. For instance, Meng et al. [10] proposed an exemplar-based algorithm to process phase dislocations before unwrapping. This method relies on modulation to detect and mask out the local structural discontinuities. Similarly, Xia et al. [8] proposed a method, referred to as PULSI+INTERP, based on combined unwrapping and inpainting by interpolation approaches for processing large dislocation areas. This method exhibits a high performance for noise-free data. However, its effectiveness is limited when dealing with high-noise levels. In this work, we propose a noise-robust approach for processing regional phase dislocations. Our approach combines phase unwrapping and sparse inpainting with dictionary learning to recover the continuous phase maps.

This paper is organized as follows. In Section 2, the theory for the proposed method is described. In Section 3, the method is validated using a simulation of strong additive white Gaussian noise and phase dislocations. An application of the proposed method in experimental data is also provided. Finally, in Section 4 we conclude and outline future work.

II. Method

An overview of the proposed approach is shown in Fig. (1). The input to the method is the wrapped phase ψ, and a binary mask $\mathbf{M}$ with ones in every pixel corresponding to a phase dislocation and zeros elsewhere. Similar to Ref [10], we use the phase modulation to obtain $\mathbf{M}$. In the first stage, $\mathbf{M}$ is applied on ψ to mask out the phase dislocation. The continuous phase map $\boldsymbol{\varphi}$ is obtained by a phase unwrapping algorithm based on least-squares and iterations referred to as PULSI [11]. We use PULSI to unwrap noise-free or low-noise phase data. However, in the presence of high-noise levels we extend our method to the calibrated version of PULSI referred to as CPULSI [12], which has proven to be more

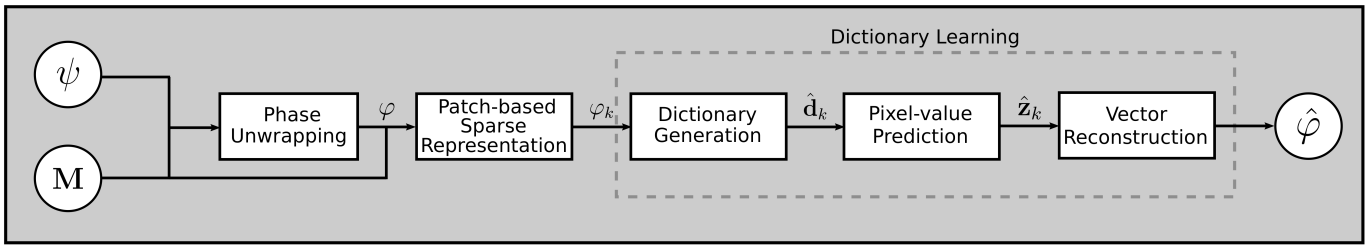

Fig. 1: Block diagram illustrating the proposed method. ψ, $\mathbf{M}$ and $\boldsymbol{\varphi}$ are the input wrapped phase, a binary mask indicating the phase dislocations and the unwrapped phase map, respectively. The restored phase is denoted as $\hat{\boldsymbol{\varphi}}$. The other variables are intermediate outputs of every stage; their meaning is given in the text.

robust than other unwrapping methods on extremely noisy phases. In the second stage, a patch-based sparse representation of $\boldsymbol{\varphi}$ is generated. In the third stage, a dictionary is trained from the image patches and starting from a predefined basis such as the Discrete Cosine Transform (DCT). $\mathbf{M}$ is used to avoid the pixels of the dislocations during the dictionary learning process. Finally, the algorithm predicts the values of the missing regions by constructing an approximate phase map $\hat{\boldsymbol{\varphi}}$. Note, $\hat{\boldsymbol{\varphi}}$ is a denoised and inpainted version of the original continuous phase map $\boldsymbol{\varphi}$. The proposed approach is referred to as PULSI+DLKSVD.

A. Sparse representation of a signal

Sparse and redundant representations are mathematical tools for modeling signals and expressing them more compactly, which leads to improvements in signal restoration [13]. In a sparse representation, an n-dimensional signal $\mathbf{y} \in \mathbb{R}^n$ is a linear combination of a small number of signals called atoms from a prespecified and redundant dictionary $\mathbf{D} \in \mathbb{R}^{n \times m}$

$$\mathbf{y} \approx \mathbf{D}\mathbf{x} \ , \tag{1}$$

where $\mathbf{x} \in \mathbb{R}^m$ is a sparse vector, i.e., $\|\mathbf{x}\|_0 << n$ being $\|.\|_0$ the ℓ_0-norm which stands for the number of non-zero elements. $\mathbf{D}$ has m elements or atoms of length n, $\mathbf{D} = [d_1, d_2, ..., d_m]$. Thus, we aim to find the sparsest representation $\mathbf{x}$, and the standard way to address this optimization problem is by imposing a sparsity constraint

$$\min_{\mathbf{x}} \|\mathbf{y} - \mathbf{D}\mathbf{x}\|_2^2, \text{ s.t. } \|\mathbf{x}\|_0 \leq T_0 \ , \tag{2}$$

where $\|.\|_2$ is the ℓ_2-norm and T_0 limits the sparsity of the representation coefficients. Note, computing the optimal solution to Eq. (2) is known to be NP-hard [14], and it is usual to replace the ℓ_0-norm by the ℓ_1-norm solved by greedy algorithms such as Orthogonal Matching Pursuit (OMP) [15], or the Least Absolute Shrinkage and Selection Operator (LASSO) [16].

B. Sparse representation based on patches

It is common to use a set of overlapping patches as the basic unit of sparse representation for images [17]–[19] with the objective of learning the sparse representation of each patch and to learn the dictionary. Let $\boldsymbol{\varphi} \in \mathbb{R}^n$ to be a vector representation of an unwrapped phase with n elements (pixels), and $\boldsymbol{\varphi}_k \in \mathbb{R}^b$ a $\sqrt{b} \times \sqrt{b}$ patch of the continuous phase in the k-th position of the $\boldsymbol{\varphi}$ vector, for $k = 1, 2, 3, ..., l$, where l is the number of patches. Moreover, let $R_k(.)$ be the operator that extracts the patches of a vector, so that $\boldsymbol{\varphi}_k = R_k(\boldsymbol{\varphi})$. Then, the transpose $R_k^T(.)$ recovers the original unwrapped phase $\boldsymbol{\varphi}$ based on the set of patches $\{\boldsymbol{\varphi}_k\}_{k=1}^l$ as

$$\boldsymbol{\varphi} = \left(\sum_{k=1}^{l} R_k^T R_k \right)^{-1} \left(\sum_{k=1}^{l} R_k^T \boldsymbol{\varphi}_k \right) \ . \tag{3}$$

With each vector patch $\boldsymbol{\varphi}_k$ and given a dictionary $\mathbf{D}$ our objective is to find the sparse vector representation $\mathbf{z}_k$ such that, based on Eq. (1), $\boldsymbol{\varphi}_k = \mathbf{D}\mathbf{z}_k$. With this condition, we are representing the phase $\boldsymbol{\varphi}$ sparsely with the set of sparse vectors $\{\mathbf{z}_k\}_{k=1}^l$ of patches of the phase, thus Eq. (3) can be rewritten as

$$\boldsymbol{\varphi} = \left(\sum_{k=1}^{l} R_k^T R_k \right)^{-1} \left(\sum_{k=1}^{l} R_k^T \mathbf{D}\mathbf{z}_k \right) \ , \tag{4}$$

where $\boldsymbol{\varphi}_k$ is replaced by $\mathbf{D}\mathbf{z}_k$.

C. Dictionary Learning

The selection of the dictionary is an important part because the sparse representation of the unwrapped phase rely on it. In the literature, there are three types of dictionaries: prebuilt, adapted, and learned dictionaries. With the latter, there have been many advances to learning a redundant dictionary from the set of training patches of the image [20] and these learned dictionaries have proven successful for inpainting and denoising. Then, the dictionary and the sparse patches are learned simultaneously with the optimization problem

$$\min_{\mathbf{D},\, \mathbf{z}_k} \sum_{k=1}^{l} \|\boldsymbol{\varphi}_k - \mathbf{D}\mathbf{z}_k\|_2^2, \text{ s.t. } \|\mathbf{z}_k\|_0 \leq T_0 \ , \tag{5}$$

where $\boldsymbol{\varphi}_k$ are each b-dimensional patch of phase $\boldsymbol{\varphi}$ represented sparsely as $\mathbf{z}_k$ with the dictionary $\mathbf{D}$. This dictionary comes from an empirical base rather than from some theoretical model being learned from the same signal, but for this learning process, a redundant prior dictionary is used. In this work, we use the discrete cosine transform (DCT) to build a prior dictionary [21], which has proven to be a plausible selection for image recovery using adaptive sparse reconstructions [22], [23].

The proposed method relies on the original continuous phase $\boldsymbol{\varphi}$ and a mask $\mathbf{M}$. The main idea of using a mask is to avoid to learn from the data that belong to the dislocation zones. In this way, $\mathbf{M}$ is a binary mask with zeros in the location of the dislocations which also indicates pixels to restore through inpainting. Using both $\boldsymbol{\varphi}$ and $\mathbf{M}$, we extract l phase patches $\boldsymbol{\varphi}_k$ and l mask patches $\mathbf{M}_k$ with the $R_k(.)$ operator, so a patch with dislocations is not used in the learning process.

In this work, we used the K-SVD algorithm to learn the dictionary and the OMP algorithm to obtain the $\mathbf{z}_k$ sparse vectors. The dictionary is updated minimizing the error

$$\mathbf{E}_k = \sum_k \|\mathbf{M}_k(\boldsymbol{\varphi}_k - \mathbf{D}\mathbf{z}_k)\|_2^2 \ . \tag{6}$$

The optimal sparse representation $\hat{\mathbf{z}}_k$ is found using a fixed atom base

$$\hat{\mathbf{z}}_k = [\mathbf{d}_m^T \mathbf{M}_k \mathbf{d}_m]^{-1} \mathbf{d}_m^T \mathbf{M}_k \boldsymbol{\varphi}_k \ . \tag{7}$$

The sparse vector is fixed, and the dictionary atoms are updated with

$$\hat{\mathbf{d}}_m = \arg\min_{\mathbf{d}_m, \mathbf{z}_k} \|R_k^T \mathbf{M}_k (\mathbf{E}_k - \mathbf{d}_m \mathbf{z}_k)\|_2^2 \ . \tag{8}$$

This process is performed iteratively until an error criterion is met or a certain amount of coefficients $\hat{\mathbf{z}}_k$ different from zero (T_0) are found to ensure a sparse representation.

D. Predicting Values and Restoration

With the sparse representation $\hat{\mathbf{z}}_k$ of all patches and the learned dictionary with the above procedure, we recover, or reconstruct, the unwrapped phase $\boldsymbol{\varphi}$ through the best approximation $\hat{\boldsymbol{\varphi}}$ using Eq. (4)

$$\hat{\boldsymbol{\varphi}} = \left(\sum_{k=1}^{l} R_k^T R_k \right)^{-1} \left(\sum_{k=1}^{l} R_k^T \hat{\mathbf{D}} \hat{\mathbf{z}}_k \right) \ , \tag{9}$$

and because there is overlapping between patches, an average reconstruction strategy is performed with this equation.

III. Experiments and Results

A. Computer simulations

We evaluated the performance of the proposed method on numerically simulated data. The MATLAB@ peaks function of 512×512 pixels is used to compute the true phase (i.e., the continuous phase). This phase is wrapped using the arctangent formula. To simulate the phase dislocations, we apply a strong moving average filter of 13×13 pixels to the sine and cosine of the wrapped phase. Then, the resulting phase map is wrapped anew into the interval $[-\pi, \pi]$. The same average filter must be applied to the original true phase to evaluate the performance of the method correctly. Fig. (2a) shows the original continuous phase, and Fig. (2b) shows the simulated wrapped phase with dislocations. Note, there are two main dislocations located in the upper and lower lobes of the phase map in Fig. (2b), where the fringe density is high compared to the size of the filtering kernel. In Fig. (2c), we show the masked areas of the dislocated phase maps. Finally, the unwrapped phase from PULSI is shown in Fig. (2d), where the masked regions are visible.

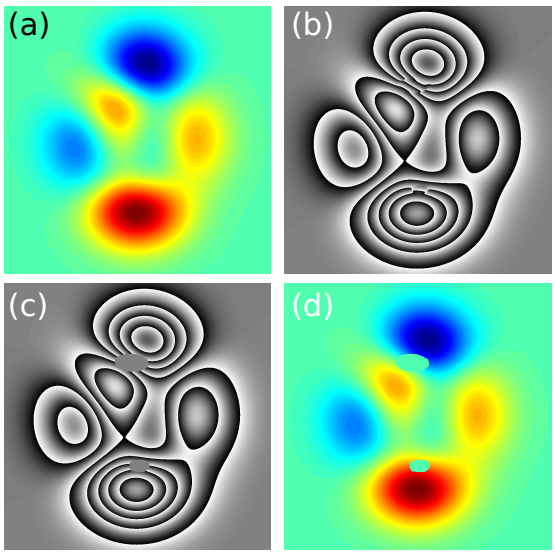

Fig. 2: (a) Original true phase, (b) wrapped phase map with dislocations, (c) masked wrapped phase, and (d) unwrapped phase from PULSI.

In Fig. (3a), we show the restored phase by applying PUSLI+DLKSVD to the phase in Fig. (2d). In order to evaluate the suitability of the proposed method, we compare our results with PULSI+INTERP in Fig. (3b). The resulting phase is in agreement with the original true phase in Fig. (2a). Fig. (3c) and Fig. (3d) show the error maps corresponding to the estimated phase regions from Fig. (3a) and Fig. (3b), respectively. For a quantitative assessment of the phase estimation quality, we computed the root-mean-square error (RMSE) in the masked areas. Here, the error given by PUSLI+DLKSVD (RMSE = 0.0170 Rad) is the lowest compared to PULSI+INTERP (RMSE = 0.0332 Rad).

To evaluate the performance of the proposed for noisy

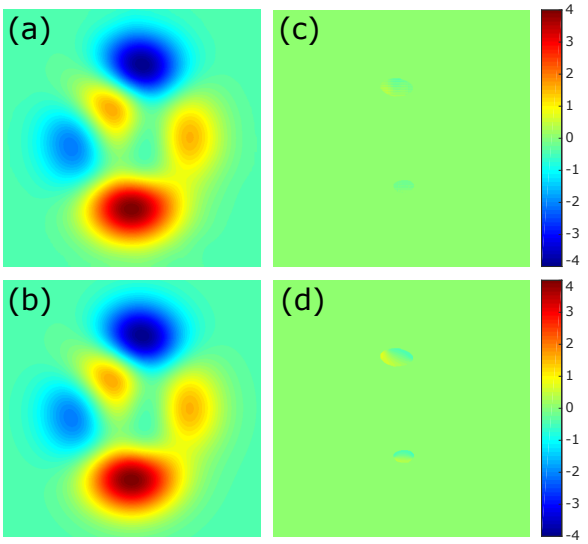

Fig. 3: Restored phases with (a) PUSLI+DLKSVD and (b) PULSI+INTER. Phase errors with (c) PUSLI+DLKSVD and (d) PULSI+INTERP.

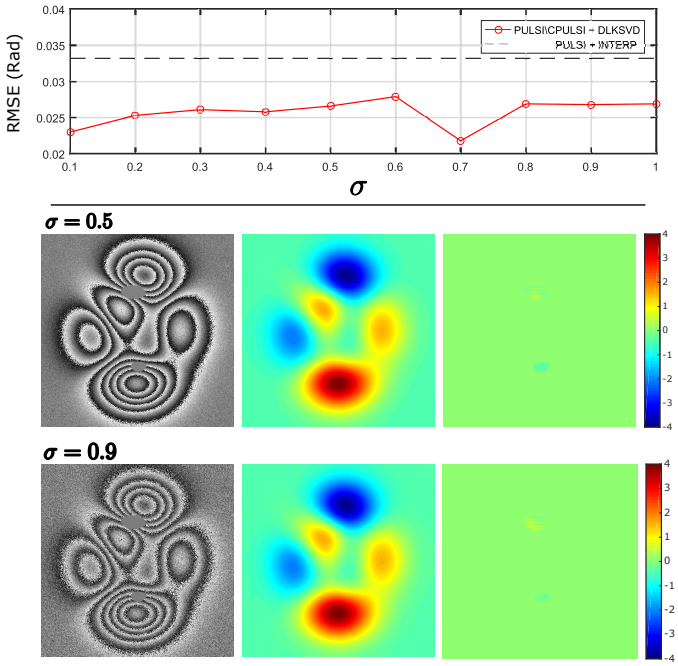

Fig. 4: Performance of the proposed for data corrupted by additive white Gaussian noise with noise standard deviation $\sigma \in \{0.1, 0.3, 0.5, 0.7, 0.9, 1.0\}$.

data, the wrapped phase map from Fig. (2b) is corrupted by additive white Gaussian noise with noise standard deviation $\sigma \in \{0.1, 0.3, 0.5, 0.7, 0.9, 1.0\}$. For $\sigma \leq 0.5$, we use PULSI for phase unwrapping. Otherwise, we use CPULSI to obtain the unwrapped phase map. The quantitative assessment of the phase restoration is shown in Fig. (4), in which we compare the obtained phase errors in the masked areas with the error from PULSI+INTERP in Fig. (3d). In addition, we show the restored phase maps for $\sigma = 0.5$, and $\sigma = 0.9$, as well as their corresponding phase errors. Note, the proposed method shows the best performance even on high noise levels.

B. Experimental verification

The proposed approach was applied to experimental phase maps obtained from human skin measurements. The experimental setup consists of two parts: a projection system and an observation system. The projection system was an LED pattern projector (Optoengineering LTPRHP3W-W) that contains a stripe pattern of 200 lines with a line thickness of 0.02 mm with a projection lens of 8-mm focal length. The observation system was a CMOS camera (Basler acA1600-60gm 1602x1202 pixels) with an objective lens of 16-mm focal length.

The object under inspection is the forearm of a test subject shown in Fig. (5a). The processing of the data is based on Fourier transform Profilometry (FTP) to extract the wrapped phase in Fig. (5b). In this application, errors can be attributed to the hair distribution which introduces local dislocations and noise to the recovered phase. The red boxes exhibit areas on which dislocations can be observed. The wrapped phase is masked and unwrapped using PULSI. The result is shown in Fig. (5c). The final restored phase with PULSI+DLKSVD is shown in Fig. (5d). As can be observed, the restoration is optimal, and the effect of the hair distribution is minimized.

Run-time of the proposed method using, e.g., a 512×512 phase map obtained from human skin measurement is $438.9423\,s$ ($7.32\,min$), including the dictionary learning process. However, we can use the learned dictionary with other similar images without having to learn a new dictionary again. Then, using another similar phase map and the same learned dictionary, computation time is approximately four times faster ($105.0148\,s$) than in the dictionary learning process.

IV. Conclusions

In this paper, we proposed a noise-robust approach for processing regional phase dislocations, based on unwrapping and sparse dictionary learning-based inpainting approaches to recover the continuous phase maps. Computer simulations, as well as experimental verification, show the suitability of the proposed method for phase restoration even in extremely noisy phases.

V. Acknowledgment

This work has been partly funded by Colciencias project 538871552485, and by Universidad Tecnológica de Bolívar projects C2018P005 and C2018P018. J. Pineda and J. Meza thank Universidad Tecnológica de Bolívar for a Masters degree scholarship.

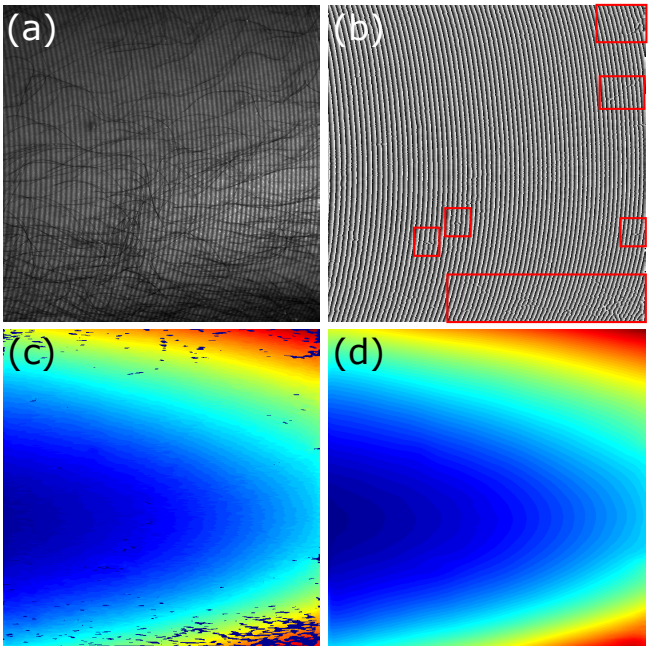

Fig. 5: (a) Captured fringe image, (b) wrapped phase map, (c) unwrapped phase from PULSI, and (d) restored phase map.

References

[1] S. S. Gorthi and P. Rastogi, "Fringe projection techniques: whither we are?," *Optics and lasers in engineering*, vol. 48, no. IMAC-REVIEW-2009-001, pp. 133–140, 2010.

[2] D. J. Bone, "Fourier fringe analysis: the two-dimensional phase unwrapping problem," *Applied optics*, vol. 30, no. 25, pp. 3627–3632, 1991.

[3] M. A. Gdeisat, D. R. Burton, F. Lilley, M. Arevalillo-Herráez, and M. M. M. Ammous, "Aiding phase unwrapping by increasing the number of residues in two-dimensional wrapped-phase distributions.," *Applied Optics*, vol. 54, pp. 10073–10078, Dec. 2015.

[4] J. Pineda, R. Vargas, L. A. Romero, J. Meneses, and A. G. Marrugo, "Fringe Quality Map for Fringe Projection Profilometry in LabVIEW," *Opt. Pura Apl.*, vol. 51, pp. 50302:1–8, Dec. 2018.

[5] M. Zhao, L. Huang, Q. Zhang, X. Su, A. Asundi, and Q. Kemao, "Quality-guided phase unwrapping technique: comparison of quality maps and guiding strategies," *Applied optics*, vol. 50, no. 33, pp. 6214–6224, 2011.

[6] J. Xu, D. An, X. Huang, and P. Yi, "An efficient minimum-discontinuity phase-unwrapping method," *IEEE Geoscience and Remote Sensing Letters*, vol. 13, no. 5, pp. 666–670, 2016.

[7] H. Yu, Y. Lan, J. Xu, D. An, and H. Lee, "Large-scale L^0 -norm and L^1 -norm 2-d phase unwrapping," *IEEE Transactions on Geoscience and Remote Sensing*, vol. 55, pp. 4712–4728, Aug 2017.

[8] H. Xia, S. Montresor, R. Guo, J. Li, F. Olchewsky, J.-M. Desse, and P. Picart, "Robust processing of phase dislocations based on combined unwrapping and inpainting approaches," *Optics letters*, vol. 42, no. 2, pp. 322–325, 2017.

[9] H. Xia, S. Montresor, P. Picart, R. Guo, and J. Li, "Comparative analysis for combination of unwrapping and de-noising of phase data with high speckle decorrelation noise," *Optics and Lasers in Engineering*, vol. 107, pp. 71–77, 2018.

[10] L. Meng, S. Fang, P. Yang, L. Wang, M. Komori, and A. Kubo, "Image-inpainting and quality-guided phase unwrapping algorithm," *Applied optics*, vol. 51, no. 13, pp. 2457–2462, 2012.

[11] H.-T. Xia, R.-X. Guo, Z.-B. Fan, H.-M. Cheng, and B.-C. Yang, "Non-invasive mechanical measurement for transparent objects by digital holographic interferometry based on iterative least-squares phase unwrapping," *Experimental mechanics*, vol. 52, no. 4, pp. 439–445, 2012.

[12] H. Xia, S. Montresor, R. Guo, J. Li, F. Yan, H. Cheng, and P. Picart, "Phase calibration unwrapping algorithm for phase data corrupted by strong decorrelation speckle noise," *Optics express*, vol. 24, no. 25, pp. 28713–28730, 2016.

[13] K. Huang and S. Aviyente, "Sparse representation for signal classification," in *Advances in neural information processing systems*, pp. 609–616, 2007.

[14] A. M. Bruckstein, D. L. Donoho, and M. Elad, "From sparse solutions of systems of equations to sparse modeling of signals and images," *SIAM review*, vol. 51, no. 1, pp. 34–81, 2009.

[15] S. Manat and Z. Zhang, "Matching pursuit in a time-frequency dictionary," *IEEE Trans Signal Processing*, vol. 12, pp. 3397–3451, 1993.

[16] R. Tibshirani, "Regression shrinkage and selection via the lasso," *Journal of the Royal Statistical Society. Series B (Methodological)*, pp. 267–288, 1996.

[17] R. Rubinstein, T. Peleg, and M. Elad, "Analysis k-svd: A dictionary-learning algorithm for the analysis sparse model," *IEEE Transactions on Signal Processing*, vol. 61, no. 3, pp. 661–677, 2013.

[18] M. Elad, J.-L. Starck, P. Querre, and D. L. Donoho, "Simultaneous cartoon and texture image inpainting using morphological component analysis (mca)," *Applied and Computational Harmonic Analysis*, vol. 19, no. 3, pp. 340–358, 2005.

[19] J. Yang, J. Wright, T. S. Huang, and Y. Ma, "Image super-resolution via sparse representation," *IEEE transactions on image processing*, vol. 19, no. 11, pp. 2861–2873, 2010.

[20] J. Zhang, D. Zhao, and W. Gao, "Group-based sparse representation for image restoration," *IEEE Transactions on Image Processing*, vol. 23, no. 8, pp. 3336–3351, 2014.

[21] T.-H. Kwok and C. C. Wang, "Interactive image inpainting using dct based exemplar matching," in *International Symposium on Visual Computing*, pp. 709–718, Springer, 2009.

[22] M. Elad and M. Aharon, "Image denoising via learned dictionaries and sparse representation," in *2006 IEEE Computer Society Conference on Computer Vision and Pattern Recognition (CVPR'06)*, vol. 1, pp. 895–900, IEEE, 2006.

[23] O. G. Guleryuz, "Nonlinear approximation based image recovery using adaptive sparse reconstructions and iterated denoising-part i: theory," *IEEE Transactions on image processing*, vol. 15, no. 3, pp. 539–554, 2006.